Transition State and Rate-Limiting Step of the Reaction Catalyzed by the Human Dual-Specificity Phosphatase, VHR†

Zhong-Yin Zhang,* Li Wu, and Li Chen

Department of Molecular Pharmacology, Albert Einstein College of Medicine, 1300 Morris Park Avenue, Bronx, New York 10461

Received July 26, 1995; Revised Manuscript Received September 28, 1995⊗

ABSTRACT: The dual-specificity phosphatases are unusual catalysts in that they can utilize protein substrates containing phosphotyrosine as well as phosphoserine/threonine. The dual-specificity phosphatases and the protein−tyrosine phosphatases (PTPases) share the active site motif (H/V)**C**(X)$_5$**R**(S/T), but display little amino acid sequence identity outside of the active site. Although the dual-specificity phosphatases and the PTPases appear to bring about phosphate monoester hydrolysis through a similar mechanism, it is not clear what causes the difference in the active-site specificity between the two groups of enzymes. In this paper, we show that the human dual-specificity phosphatase, VHR [for VH1-Related; Ishibashi et al. (1992) *Proc. Natl. Acad. Sci. U.S.A. 89,* 12170−12174], is rather promiscuous toward small phosphate monoesters (including both aryl and alkyl phosphates of primary alcohols) with effectively identical k_{cat}/K_m and k_{cat} values while the pK_a values of the leaving groups (phenols or alcohols) varied from 7 to 16. Linear free-energy relationship analysis of k_{cat} and k_{cat}/K_m of the enzyme-catalyzed hydrolysis reaction suggests that a uniform mechanism is utilized for both the aryl and alkyl substrates. The very small dependency of k_{cat}/K_m on the leaving group pK_a can be accounted for by the protonation of the leaving group. Pre-steady-state burst kinetic analysis of the VHR-catalyzed hydrolysis of *p*-nitrophenyl phosphate provides direct kinetic evidence for the involvement of a phosphoenzyme intermediate in the dual specificity phosphatase−catalyzed reaction. The rate-limiting step for the VHR-catalyzed hydrolysis of *p*-nitrophenyl phosphate corresponds to the decomposition of the phosphoenzyme intermediate. Results from kinetic solvent isotope effects on the formation ($k^{H_2O}/k^{D_2O} = 0.52$) and the breakdown ($k^{H_2O}/k^{D_2O} = 1.15$) of the phosphoenzyme intermediate are consistent with a highly dissociative metaphosphate-like transition state for both steps, where bond formation to the incoming nucleophile is minimal and bond breaking between phosphorus and the leaving group is substantial. To promote and stabilize the dissociative transition state, the proton from the putative general acid Asp92 is largely transferred to the bridge oxygen atom in the transition state.

Protein tyrosine phosphatases (PTPases) play an important role in cellular signal transductions (Fischer et al., 1991; Charbonneau & Tonks, 1992; Walton & Dixon, 1993). PTPases constitute a growing family of enzymes that can be divided into two groups, receptor-like and intracellular PTPases. Although many PTPases are proteins of greater than 400 amino acids, their catalytic domains are usually contained within a span of 250 residues referred to as the PTPase domain. This domain is the only structural element that has amino acid sequence identity among all PTPases from bacteria to mammals (Zhang et al., 1994a). PTPases show no sequence similarity with serine/threonine phosphatases, or the broad-specificity phosphatases such as acid or alkaline phosphatases. The unique feature that defines the whole PTPase family is the active-site sequence (H/V)-**C**(X)$_5$**R**(S/T) in the catalytic domain called the PTPase signature motif (Zhang et al., 1994b).

Recently, another group of enzymes, called dual-specificity phosphatases, has been delineated. This group includes the *vaccinia* phosphatase, VH1, (for *Vaccinia* open reading frame *H1*) (Guan et al., 1991), the cell cycle regulator cdc25 (Gautier et al., 1991), and a number of mammalian dual-specificity phosphatases that are capable of dephosphorylating and inactivating mitogen-activated kinase (MAP kinase) (Sun et al., 1993; Ward et al., 1994). Unlike the PTPases which show substrate specificity strictly restricted to phosphotyrosyl proteins (Sparks & Brautigan, 1985; Tonks et al., 1988; Guan & Dixon, 1990), this group of phosphatases are unusual in that they can utilize substrates containing phosphotyrosine, phosphoserine, and phosphothreonine (Gautier et al., 1991; Guan et al., 1991; Ishibashi et al., 1992). Interestingly, the VH1-like dual-specificity phosphatases and the tyrosine-specific PTPases share the active-site motif (H/V)**C**(X)$_5$**R**(S/T) but display little amino acid sequence identity outside of the active site. It appears that both the dual-specificity phosphatases and the PTPases bring about phosphate monoester hydrolysis through a novel phosphocysteine intermediate involving the active-site cysteine residue (Guan & Dixon, 1991; cho et al., 1992; Wo et al., 1992; Zhou et al., 1994).

Although PTPases and dual-specificity phosphatases likely utilize a common catalytic mechanism for phosphate mo-

† This work was supported partially by a grant from NIH (DRTC 5P60 DK20541-17) to Z.-Y. Z.

* To whom correspondence should be addressed: Department of Molecular Pharmacology, Albert Einstein College of Medicine, 1300 Morris Park Av., Bronx, NY 10461. Tel.: 718-430-4288. Fax: 718-430-8922.

⊗ Abstract published in *Advance ACS Abstracts,* December 1, 1995.

0006-2960/95/0434-16088$09.00/0

noester hydrolysis, a detailed understanding of their active-site substrate specificity is lacking. PTPases are believed to exhibit a restricted specificity toward phosphotyrosine. Such discriminatory behavior is expected, given the differences in orientation and distance of the phosphate moiety, relative to the adjacent peptide backbone, in phosphotyrosine compared to those in phosphoserine/threonine. The unique structural features that enable the dual-specificity phosphatases to work on both phosphotyrosyl and phosphoseryl/threonyl proteins are not known. In this study, we explore the active-site specificity of the human dual-specificity phosphatase, VHR (for VH1-Related) (Ishibashi et al., 1992), which may be responsible for activation of cdk−cyclin complex(es) at some stage of the cell cycle (Aroca et al., 1995). We find that VHR is rather promiscuous toward phosphate monoesters. Thus, the VHR-catalyzed hydrolysis of alkyl phosphates exhibits k_{cat} values that are similar to those of aryl phosphates. It appears that the major difference between the PTPases and the dual-specificity phosphatases is that the latter has evolved to stabilize the developing negative charge on the leaving alkoxide or phenoxide with equal efficiency, thus possessing higher intrinsic activity toward alkyl phosphates. We have demonstrated pre−steady-state burst kinetics with VHR using *p*-nitrophenyl phosphate (*p*NPP) as a substrate, suggesting that the rate-limiting step for k_{cat} is the decomposition of the phosphoenzyme intermediate. We have also conducted a kinetic solvent isotope effect study on both the formation and the breakdown of the phosphoenzyme intermediate. Surprisingly, a sizable inverse D_2O solvent kinetic isotope effect is associated with the formation of the intermediate, whereas a small normal isotope effect is observed with the breakdown of it. Mechanistic models are advanced concerning the nature of the transition state of the enzyme-catalyzed reaction.

EXPERIMENTAL PROCEDURES

Materials. *p*-Nitrophenyl phosphate (*p*NPP), β-naphthyl phosphate, *O*-phospho-L-tyrosine, *O*-phospho-L-serine, *O*-phospho-L-threonine, pyridoxal 5′-phosphate, D-glucose 6-phosphate, α-D-glucose 1-phosphate, DL-α-glycerophosphate, and *O*-phosphorylethanolamine were purchased from Sigma. Alkyl phosphate monoesters having a pendant aromatic group [$Ar(CH_2)_nOPO_3H_2$, $n = 1-5$] were synthesized and characterized as described earlier (Zhang & Van Etten, 1990). Deuterium oxide (99.9%) was obtained from Sigma. Solutions were prepared using deionized and distilled water. The cDNA encoding the human dual-specificity phosphatase, VHR, was obtained using the polymerase chain reaction (PCR) from a human fetal brain cDNA library (Stratagene). The PCR primers and the detailed procedures for obtaining the VHR coding sequence and its subsequent subcloning into the plasmid pT7-7 were described in Zhou et al. (1994). Homogeneous recombinant human VHR was expressed and purified using a procedure similar to that described previously (Denu et al., 1995a).

Steady-State Kinetics. Initial rates for the enzyme-catalyzed hydrolysis of phosphate monoesters were measured at 30 °C by the production of inorganic phosphate using a colorimetric method described earlier (Zhang & Van Etten, 1991a; Black & Jones, 1983). Eight different substrate concentrations ranging from 0.16 to 8 K_m were used to obtain the K_m and k_{cat} data in two independent experiments. Control samples (without the addition of enzyme) were prepared in order to correct for spontaneous hydrolysis and the presence of small amounts of phosphate in the substrates. Buffers used were as follow: pH 5.0, 100 mM acetate; pH 6.0, 50 mM succinate; and pH 7.0, 50 mM 3,3-dimethylglutarate. All of the buffer systems contained 1 mM EDTA, and the ionic strength of the solutions were kept at 0.15 M using NaCl. Michaelis−Menten kinetic parameters were determined from a direct fit of the v vs. [S] data to the Michaelis−Menten equation using the nonlinear regression program GraFit (Erithacus Software).

Rapid Kinetics. Pre−steady-state kinetic measurements of the VHR-catalyzed hydrolysis of *p*NPP were conducted using a Hi-Tech SF-61 stopped-flow spectrophotometer (dead time, 2 ms) with an observation cell length of 1.0 cm. Fast reactions at 30 °C were monitored by the increase in absorbance at 410 nm of the *p*-nitrophenolate product. The final *p*NPP concentration was 20 mM (10-fold higher than the K_m) and the concentration of VHR was 113 μM. The extinction coefficient for *p*-nitrophenolate at 410 nm is 1325 M^{-1} cm^{-1} at pH 6.0 and 30 °C. The enzyme concentration was determined from the absorption at 280 nm using an absorption coefficient of 11 500 M^{-1} cm^{-1} (Denu et al., 1995a). When VHR and *p*NPP are rapidly mixed in a stopped-flow spectrophotometer, the increase in *p*-nitrophenolate concentration as a function of time can be described as [*p*-nitrophenolate] $= At + B(1 - e^{-bt}) + C$ (Zhang & Van Etten, 1991a; Zhang, 1995a). When the experiments are performed at saturating concentrations of substrate, the individual rate constants for the enzyme phosphorylation (k_2) and dephosphorylation (k_3) can be determined from the exponential ($b = k_2 + k_3$) and the linear phase [$A = k_2k_3/(k_2 + k_3)$], respectively (Scheme 1). The size of the burst $B = E_o[k_2/(k_2 + k_3)]^2/(1 + K_m/S_o)^2$ and is proportional to the active enzyme concentration.

Denu et al. (1995b) recently performed a pre−steady-state kinetic analysis of the VHR-catalyzed hydrolysis of *p*NPP, and were unable to observe a burst of *p*-nitrophenolate formation at 405 nm, pH 7 and 30 °C. We have employed identical procedures in obtaining homogeneous recombinant VHR. The steady-state kinetic parameters determined in our laboratory using *p*NPP agree well with those determined by Denu et al. (1995a,b). The rate of the VHR-catalyzed reaction is not particularly fast and is certainly within the detection limit of a modern stopped-flow spectrophotometer. It is not clear what causes the disparity in the stopped-flow experiments. We noticed however that the K_m value for *p*NPP at pH 7.0 and 30 °C is 7.85 mM (Tale 2, this study) which is similar to the previously reported value of 7.99 mM (Denu et al., 1995a). In order to observe burst kinetics, one would have to saturate the enzyme with substrate. Denu et al. (1995b) used up to 50 mM *p*NPP in their stopped-flow experiments at pH 7.0. Since *p*NPP itself also absorbs at 405 nm, the background due to the presence of high substrate concentration would be so enormous that observation of a meaningful burst would be technically difficult (Zhang & Van Etten, 1991a). Differences in the buffer systems used may be another contributing factor.

D_2O Solvent Isotope Effect. Both the pre−steady-state and steady-state solvent kinetic isotope experiments were conducted in the equivalent buffer of pH 6.0, 50 mM succinate, 1 mM EDTA, I = 0.15 M (Quinn & Sutton, 1991). Buffered solutions of heavy water (100 mL) were prepared as follows: 100 mL of pH 6.0 buffer was lyophilized to

Table 1: VHR Hydrolyzes both Aryl and Alkyl Phosphates Rather Indiscriminately

substrate	pK_a of leaving group	k_{cat} (s^{-1})	K_m (mM)	k_{cat}/K_m (M^{-1} s^{-1})
p-nitrophenyl phosphate	7.14[a]	5.97 ± 0.24	1.94 ± 0.23	3080
4-methyl umbelliferyl phosphate	7.80[b]	6.74 ± 0.31	0.72 ± 0.11	9360
β-naphthyl phosphate	9.38[a]	6.80 ± 0.41	0.50 ± 0.07	13600
phenyl phosphate	9.99[a]	6.65 ± 0.09	1.57 ± 0.11	4230
O-phospho-L-tyrosine	10.07[a]	5.87 ± 0.37	2.20 ± 0.38	2670
pyridoxal-5′-phosphate	13[c]	3.99 ± 0.15	3.50 ± 0.45	1140
benzyl phosphate $ArCH_2OPO_3H_2$	14.84[a]	5.23 ± 0.30	5.13 ± 0.63	1020
2-phenylethyl phosphate $Ar(CH_2)_2OPO_3H_2$	15.59[a]	5.33 ± 0.60	4.21 ± 0.70	1270
3-phenylpropyl phosphate $Ar(CH_2)_3OPO_3H_2$	15.79[a]	5.89 ± 0.22	3.64 ± 0.33	1620
4-phenylbutyl phosphate $Ar(CH_2)_4OPO_3H_2$	15.87[a]	3.96 ± 0.41	2.29 ± 0.30	1720
5-phenylpentyl phosphate $Ar(CH_2)_5OPO_3H_2$	15.9[a]	4.97 ± 0.25	2.40 ± 0.33	2070
D-glucose-6-phosphate	12.4[d]	2.80 ± 0.49	103 ± 20	27
DL-α-glycerophosphate	14.4[d]	2.73 ± 0.18	53.4 ± 4.5	51
α-D-glucose-1-phosphate	12.4[d]	0.292 ± 0.078	56.5 ± 18	5.2
O-phosphorylethanolamine	~14[e]	0.480 ± 0.059	52.6 ± 7.7	9.1
O-phospho-L-serine	~14[e]	0.158 ± 0.043	31.3 ± 10.7	5.0
O-phospho-L-threonine	~14[e]	1.54 ± 0.15	21.7 ± 0.28	71

[a] Zhang and Van Etten (1991b); [b] Zhang (1995b); [c] Perrin (1965); [d] Ballinger and Long (1960); [e] estimated from the pK_a value of choline.

dryness. It was then redissolved in 20 mL of D_2O and lyophilized to dryness. This process was repeated for another time. Finally, all of the buffer components were reconstituted in 100 mL of D_2O. As predicted by theory, the pH meter reading of the buffered D_2O solution was 6.10, which was 0.10 pH units greater than the pH of the corresponding buffer in H_2O (Quinn & Sutton, 1991). Thus the corresponding pD value = pH meter reading + 0.4 = 6.50. Solutions prepared in this manner ensure that reactions are studied at equivalent positions on the pH−rate profiles in the isotopic solvents. The extinction coefficient at 410 nm for *p*-nitrophenolate is 1250 M^{-1} cm^{-1} in this buffer. Slow or irreversible changes in enzyme activity as a result of the presence of D_2O were ruled out by the linear time courses obtained in H_2O and D_2O buffers and by assaying identical stock solutions of VHR prepared in H_2O and D_2O in water after prolonged incubation for days. Similar steady-state kinetic parameters were obtained when the assays are conducted in either H_2O buffer or D_2O buffer.

RESULTS AND DISCUSSION

The Dual-Specificity Phosphatase, VHR, Is Promiscuous toward Phosphate Monoesters. Activity of dual specificity phosphatases toward both phosphotyrosine and phosphoserine/threonine is abolished when the active-site cysteine nucleophile is replaced with serine, suggesting that the hydrolysis of both phosphotyrosyl and phosphoseryl/threonyl peptides/proteins proceeds *via* the same active site (Sun et al., 1993; Zhou et al., 1994). Since the VH1-like dual-specificity phosphatases and the tyrosine-specific PTPases share the active-site motif (H/V)**C**(X)$_5$**R**(S/T) and apparently utilize a similar mechanism for phosphate monoester hydrolysis, it is not clear how the dual-specificity phosphatases manage to operate on both phosphotyrosyl and phosphoseryl/threonyl peptide/protein substrates. A detailed kinetic study of the dual-specificity phosphatases using more physiological protein substrates is not feasible because of the difficulty in preparing large amount of stoichiometrically phosphorylated proteins. In this study, we employed homogeneous recombinant VHR as a model for the dual-specificity phosphatases, and explored its active-site specificity in terms of the range of functionality that can be accommodated within the active site. We examined VHR's ability to hydrolyze a variety of small aryl and alkyl phosphate monoesters. As expected, VHR catalyzed the hydrolysis of a variety of alkyl phosphate monoesters such as pyridoxal 5′-phosphate, D-glucose 6-phosphate, DL-α-glycerophosphate, *O*-phospho-L-serine and *O*-phospho-L-threonine. The amount of inorganic phosphate generated was proportional to the amount of VHR present and the duration of the reaction. The hydrolysis of both aryl and alkyl phosphates can be effectively blocked by the presence of 3 mM vanadate, a good competitive inhibitor of VHR (Denu et al., 1995a). This is consistent with the notion that the dual-specificity phosphatases catalyze the hydrolysis of aryl and alkyl phosphates *via* the same active site.

Table 1 summarizes the Michaelis−Menten kinetic parameters of VHR at pH 6.0 and 30 °C toward aryl and alkyl phosphates. We have demonstrated recently that PTPases, which display restricted specificity toward phosphotyrosyl proteins, also hydrolyze small alkyl phosphates (Zhang, 1995b). However, the PTPases-catalyzed hydrolysis of alkyl phosphates are much slower (10^2 to 10^3 fold) than that of aryl phosphates. In contrast to PTPases, VHR hydrolyzes aryl and alkyl phosphates rather indiscriminately. For example, VHR dephosphorylate aryl phosphates such as *p*NPP and tyrosine phosphate with turnover numbers similar to those of alkyl phosphates of primary alcohols such as pyridoxal 5′-phosphate, 5-phenylpentyl phosphate, D-glucose 6-phosphate, and DL-α-glycerophosphate. Consistent with the phosphorylation reaction being nucleophilic in nature, alkyl phosphates of secondary alcohols such as α-D-glucose 1-phosphate or primary alcohols with β-substituted positive charges and/or side chains such as *O*-phospho-L-serine and *O*-phosphorylethanolamine are poorer substrates (12 to 38 times slower) than esters of primary alcohols. The lower reactivity with secondary alcohols could also result from differences in binding and positioning. Interestingly, *O*-phospho-L-threonine, which is a secondary alkyl phosphate, exhibits a k_{cat} value that is 10-fold higher than that of *O*-phospho-L-serine, and approaches those of aryl phosphates (Table 1). We do not know why VHR shows enhanced reactivity toward *O*-phospho-L-threonine as opposed to *O*-phospho-L-serine.

Leaving Group Dependence. Since a cysteinyl phosphate covalent enzyme intermediate is involved in the VHR-catalyzed reactions, the minimal kinetic mechanism can be

Scheme 1

$$E + ROPO_3^{2-} \underset{k_{-1}}{\overset{k_1}{\rightleftharpoons}} E \bullet ROPO_3^{2-} \xrightarrow{k_2} E - P \xrightarrow{k_3} E + P_i$$
$$\downarrow$$
$$ROH$$

illustrated by Scheme 1. In the first catalytic step (k_2), the VHR-catalyzed hydrolysis of phosphate monoesters involves the attack of the phosphorus atom by the active site Cys124 (Zhou et al., 1994), forming the thiophosphate intermediate (E-P) with the release of ROH, the leaving group phenol/alcohol. In the second step (k_3), the hydrolysis of the phosphoenzyme intermediate would require water to attack the phosphorus atom, thus regenerating the active-site nucleophile and yielding the other product of the reaction, inorganic phosphate. We were struck by the observation that the VHR-catalyzed hydrolysis of phosphate monoesters (including both aryl and alkyl phosphates of primary alcohols) exhibited effectively similar k_{cat} values while the pK_a values of the leaving groups (phenols or alcohols) varied from 7 to 16 (Table 1). In general, nonspecific phosphatases, such as alkaline and acid phosphatases, exhibit the lack of dependence of k_{cat} on the pK_a of the leaving group. It is interesting to note that alkyl phosphates having a pendant aromatic group, such as pyridoxal 5′-phosphate and compounds with the structure $Ar(CH_2)_nOPO_3H_2$ ($n = 1-5$), have K_m values similar to those of aryl phosphates, suggesting that the aromatic moieties are important for VHR binding. The fact that similar kinetic parameters are observed for substrates with 0 to 5 methylene units between the phosphate and the aromatic moiety also indicates that the active site of VHR is rather flexible. Although the k_{cat} values for alkyl phosphates of primary alcohols are similar to those of the aryl phosphates, the fact that their K_m values are much higher than the aryl phosphates suggests that they may fall into a different class of substrates. We therefore performed a linear free-energy relationship (Brønsted correlation) analysis of the VHR-catalyzed hydrolysis of aryl phosphates and alkyl phosphates with an aromatic moiety attached to the aliphatic chain.

Figure 1A and 1B show the Brønsted plots that relate the k_{cat} and k_{cat}/K_m values, respectively, to the pK_a values of the leaving group for *p*NPP, 4-methyl umbelliferyl phosphate, β-naphthyl phosphate, phenyl phosphate, phosphotyrosine, pyridoxal 5′-phosphate, benzyl phosphate, 2-phenylethyl phosphate, 3-phenylpropyl phosphate, 4-phenylbutyl phosphate, and 5-phenylpentyl phosphate. The β_{lg} for k_{cat} [which is the slope of log(k_{cat}) versus pK_a] is -0.015 ± 0.006, whereas the β_{lg} for k_{cat}/K_m [which is the slope of log(k_{cat}/K_m) versus pK_a] is -0.074 ± 0.023. Thus, there is effectively a very small leaving-group effect on catalysis for both k_{cat}/K_m and k_{cat}. The linear relationships suggest that the transition-state structures are similar for all of these substrates and that a uniform mechanism is utilized over the wide range of pK_a values.

As shown in Scheme 1, the kinetic parameter $k_{cat} = k_2k_3/(k_2 + k_3)$ and provides information on both the formation (k_2) and the breakdown (k_3) of the intermediate. One would normally predict that (a) if the rate-limiting step is the formation of the intermediate (k_2), a leaving-group effect on k_{cat} should be observed; and (b) if the rate-limiting step is the breakdown of the intermediate (k_3), no leaving-group effect should be observed. The fact that the VHR-catalyzed hydrolysis of aryl and alkyl phosphates, substrates that differ markedly in their leaving-group pK_a (for example, 7.14 for *p*-nitrophenol and 15.9 for 5-phenylpentanol), display identical k_{cat} values is consistent with the rate-determining step being the breakdown of the phosphoenzyme intermediate. To substantiate this conclusion, we also measured the kinetic parameters for both aryl phosphates and alkyl phosphates at pH 5.0 and 7.0 (Table 2). Again, the k_{cat} values for the VHR-catalyzed hydrolysis of alkyl phosphates are similar to those of aryl phosphates at both pH values, consistent with a rate-limiting hydrolysis of the phosphoenzyme intermediate.

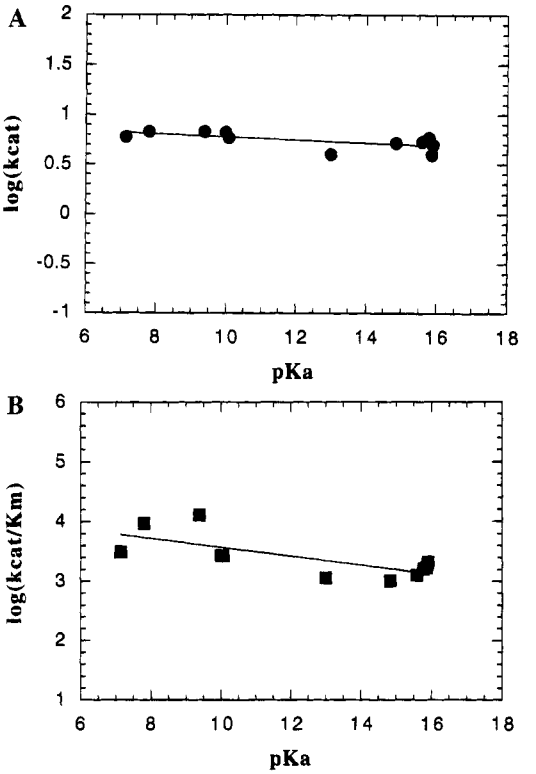

FIGURE 1: Leaving-group dependence of the VHR-Catalyzed phosphate monoester hydrolysis. (A and B) Leaving group dependence of k_{cat} and k_{cat}/K_m, respectively. Compounds that are included in the plots are *p*NPP, 4-methyl umbelliferyl phosphate, β-naphthyl phosphate, phenyl phosphate, phosphotyrosine, pyridoxal 5′-phosphate, benzyl phosphate, 2-phenylethyl phosphate, 3-phenylpropyl phosphate, 4-phenylbutyl phosphate, and 5-phenylpentyl phosphate. The lines that are drawn through the experimental data are generated by a linear regression method.

The kinetic parameter $k_{cat}/K_m = k_1k_2/(k_{-1} + k_2)$ and involves binding of substrate (k_1 and k_{-1}) through the first irreversible step in the overall reaction, which most likely corresponds to the formation of the intermediate and the release of the phenol or alcohol leaving group (k_2). It is unlikely that the binding kinetics for this group of substrates would differ significantly since they all have similar K_m values. Substrate binding is probably not rate-limiting, given the low k_{cat}/K_m values (Table 1). Thus, we assume k_{cat}/K_m monitors mainly the formation of the phosphoenzyme. A small β_{lg} value (-0.074 ± 0.023) is observed for k_{cat}/K_m which is most consistent with an electrophilic interaction between the enzyme active site and the oxygen atom of the leaving group. In fact, such a low sensitivity to leaving-group dependence in the phosphate monoester monoanion hydrolysis has been attributed to the protonation of the leaving group (Kirby & Varvoglis, 1967). It is remarkable that the catalytic machinery of VHR neutralizes the developing negative charge on the leaving groups with proton

Table 2: pH Dependencies of Kinetic Parameters for the VHR-Catalyzed Phosphate Monoester Hydrolysis

	pH 5.0		pH 6.0		pH 7.0	
substrate	k_{cat} (s^{-1})	K_m (mM)	k_{cat} (s^{-1})	K_m (mM)	k_{cat} (s^{-1})	K_m (mM)
p-nitrophenyl phosphate	4.25 ±0.11	3.07 ±0.23	5.97 ±0.24	1.95 ±0.23	4.42 ±0.08	7.85 ±0.28
β-naphthyl phosphate	4.85 ±0.06	0.60 ±0.02	6.80 ±0.41	0.50 ±0.07	6.75 ±0.13	1.16 ±0.07
O-phospho-L-tyrosine	4.71 ±0.48	7.42 ±1.2	5.87 ±0.37	2.20 ±0.38	4.74 ±0.53	7.36 ±1.45
5-phenylpentyl phosphate	1.65 ±0.06	2.56 ±0.52	4.97 ±0.25	2.40 ±0.33	6.22 ±0.23	4.26 ±0.47
pyridoxal-5′-phosphate	1.35 ±0.07	6.01 ±0.62	3.99 ±0.15	3.50 ±0.45	2.28 ±0.08	11.2 ±0.78

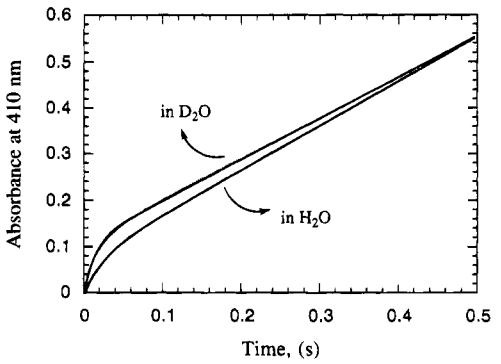

FIGURE 2: Burst kinetics observed with VHR and *p*NPP at 30 °C in H_2O and D_2O. Each stopped-flow trace was an average of at least 6 individual experiments. The solid line represents a theoretical fit of the data to the equation [*p*-nitrophenolate] = $At + B(1 - e^{-bt}) + C$. In experiments performed in pH 6.0 buffer in H_2O, the VHR enzyme concentration was 113 μM and the *p*NPP concentration was 20 mM. In experiments performed in pD 6.5 (equivalent buffer of the pH 6) buffer in D_2O, the VHR enzyme concentration was 120 μM and the *p*NPP concentration was 20 mM.

affinities that differ by as much as 9 orders of magnitudes equally well! This could be the reason that the dual-specificity phosphatases dephosphorylate aryl and alkyl phosphates rather indiscriminately.

If the assumption that the kinetic parameter k_{cat}/K_m provides information on the phosphoenzyme intermediate formation in the VHR-catalyzed reaction is correct, one could not tell which step is rate-limiting for the entire enzymatic reaction based purely on the leaving-group dependence data. As discussed above, a rate-limiting intermediate formation would certainly be consistent with the data if the enzyme stabilizes the leaving group with differing pK_a values equally well. In order to resolve this issue unambiguously, we turned to rapid kinetic techniques.

The Rate-Limiting Step. We have performed a pre-steady-state stopped-flow kinetic analysis of the VHR-catalyzed hydrolysis of *p*NPP at pH 6.0 and 30 °C (Figure 2). Analysis of the time course obtained permits calculation of rate constants associated with the kinetically distinguishable elementary steps, *i.e.*, the formation and the breakdown of the phosphoenzyme intermediate, and thus provides information that is unobtainable by steady-state techniques. By varying the initial concentration of the enzyme and the substrate, we found that the amplitude of the burst is proportional to the enzyme concentration and that the dependency of the burst size on the substrate concentration can be adequately described by $B = E_o[k_2/(k_2 + k_3)]^2/(1 + K_m/S_o)^2$. For example, the experimentally determined burst for VHR at pH 6.0 and 20 mM *p*NPP (113 μM VHR, Figure 2) was 58.8 μM and corresponded to 52% of the enzyme concentration. The steady-state kinetic parameters (determined independently of the stopped-flow experiments) at 30 °C and pH 6.0 using *p*NPP as a substrate were $k_{cat} = 5.97$ s^{-1} and $K_m = 1.95$ mM. The individual rate constant for the intermediate formation (k_2) and breakdown (k_3) were determined from the following relationships: $b = k_2 + k_3 = 41.7$ s^{-1} and $A = k_2k_3/(k_2 + k_3) = 6.26$ s^{-1}. Thus, k_2 and k_3 were determined as 34.0 s^{-1} and 7.6 s^{-1}, respectively. The theoretical burst calculated from these values is 55% of the enzyme active site concentration at 20 mM *p*NPP. Thus there is good agreement between the directly observed amplitude of the burst with the theoretically predicted value based on the experimental conditions.

Product (*p*-nitrophenol or inorganic phosphate) dissociation is unlikely to be rate-limiting for the overall reaction. This conclusion can be drawn from the following consideration. Assuming an association rate constant for inorganic phosphate, k_{on}, of 10^6–10^8 M^{-1} s^{-1} (Hammes & Schimmel, 1970), the dissociation rate constant k_{off} can be calculated [from $k_i = k_{off}/k_{on} = 0.97$ mM for inorganic phosphate (Denu et al., 1995a)] as $9.7 \times 10^2 - 9.7 \times 10^4$ s^{-1} at pH 6.0 and 30 °C. This is much greater than the maximum turnover number (5.97 s^{-1}) for the VHR-catalyzed *p*NPP hydrolysis under the same conditions. *p*-Nitrophenol is a much poorer inhibitor of PTPases (Zhang et al., 1994c; Zhang, 1995a), suggesting that dissociation of *p*-nitrophenol from the active site is even more rapid and therefore not rate-limiting. Overall, these results establish that the rate-limiting step of the VHR-catalyzed hydrolysis of phosphate monoesters is k_3, the decomposition of the phosphoenzyme intermediate.

Since k_3 is only 4.5-fold slower than k_2, if there is a strong leaving-group effect on the k_2 step, one would also see it on k_{cat} [which is $k_2k_3/(k_2 + k_3)$]. The fact that k_{cat} displays little leaving-group dependence also suggests that k_2 has minimal leaving-group dependence. Indeed, burst kinetics is also observed when 4-methyl umbelliferyl phosphate or β-naphthyl phosphate is used as substrate with k_2 values similar to that of *p*NPP (unpublished results). Thus our assumption that k_2 and k_{cat}/K_m in fact follow the same catalytic step is likely to be correct. Demonstration of burst kinetics with VHR provides direct kinetic evidence for the involvement of a phosphoenzyme intermediate in dual-specificity phosphatase catalysis. More importantly, this approach combined with the technique of site-directed mutagenesis should allow one to ascertain specific contributions of active-site amino acid side-chains to the individual steps of the dual-specificity-phosphatase–catalyzed reaction.

Kinetic Solvent Isotope Effect. In addition to nucleophilic catalysis, it appears that both PTPases and the dual-specificity phosphatases also utilize general acid/base to facilitate the enzymatic reaction. For example, an invariant Asp residue (Asp356 in the *Yersinia* PTPase) has been suggested to function as a general acid in the catalytic mechanism of the PTPases by a combination of site-directed mutagenesis and pH−rate profile analysis (Zhang et al., 1994a). In the *Yersinia* PTPase, Asp356 is found on a flexible loop that undergoes a major conformational change upon binding of tungstate (Stuckey et al., 1994). This loop movement brings Asp356 into a position to act as a general acid to facilitate the departure of the leaving group. Similarly, a conserved Asp residue in the dual-specificity phosphatases (Asp92 in VHR) has also been proposed to play the role of a general acid (Denu et al., 1995b). The common catalytic strategy shared by the two classes of enzymes is likely to involve the Cys residue acting as the nucleophile to attack the phosphate ester, forming a thiophosphate intermediate, while the active-site Asp residue acts as a general acid donating a proton to the leaving group to assist its departure. The hydrolysis of the phosphoenzyme intermediate is likely to be facilitated by the same Asp residue which now acts as a general base activating a water molecule.

In order to examine whether a proton-transfer process occurs in the transition states of phosphoenzyme formation and breakdown, we measured the kinetic solvent isotope effect of the VHR-catalyzed reaction. The experiments were conducted at equivalent pL value (pH 6.0 in 50 mM succinate, 1 mM EDTA, I = 0.15 M, and pD 6.5 in the equivalent buffer of the former, see Experimental Procedures) and the plateau region of the pH−rate profile (Denu et al., 1995b), to avoid necessarily imprecise corrections for isotope effects on essential ionizations. Figure 2 compares the complete burst kinetic time course of the VHR-catalyzed hydrolysis of *p*NPP in D_2O buffer as well as in H_2O buffer at 30 °C. We found that in the presence of D_2O, the experimentally determined burst for VHR at pD 6.5 and 20 mM *p*NPP (120 μM VHR, Figure 2) was 93.4 μM and corresponded to 78% of the enzyme concentration. The rate constants for the exponential (b) and the linear phase (A) were determined to be 71.7 s^{-1} and 5.95 s^{-1}, respectively. Thus, the individual rate constant for the intermediate formation (k_2) and breakdown (k_3) were calculated to be 65.1 s^{-1} and 6.6 s^{-1}. The theoretical burst calculated from these values is 73% of the enzyme active-site concentration. Again there is good agreement between the directly observed amplitude of the burst with the theoretically predicted value based on the experimental conditions. The burst is more pronounced in D_2O due to the increase in the ratio of k_2/k_3.

When protons are transferred or "in-flight" in the transition state of the rate-limiting step of a reaction pathway, normal solvent isotope effects ($k^{H_2O}/k^{D_2O} > 2$) are expected. We observed an inverse kinetic solvent isotope effect on k_2 of 0.52 and a normal kinetic solvent isotope effect on k_3 of 1.15. Inverse solvent isotope effects on enzyme-catalyzed reactions are rare and have generally been explained by the assumption that protonation equilibria involving acids with low fractionation factors precede the rate-limiting step in catalysis. In such a case the inverse pre-equilibrium effect may cancel a small normal effect in the subsequent rate-limiting step (Klinman, 1977). Among species with low fractionation factors are sulfhydryl groups and metal-coordinated water molecules (Schowen & Schowen, 1982). VHR is not a metalloenzyme but involves an active-site Cys residue in catalysis (Zhao et al., 1994). It has been shown that the alkylating reagent iodoacetate can selectively carboxymethylate the active site Cys124 (Zhao et al., 1994). We observed no significant solvent isotope effect in the alkylation reaction. There was also no solvent isotope effect in the alkylation of the active-site Cys residue in the *Yersinia* PTPase (Zhang & Dixon, 1993). Furthermore, since the transition state is dissociative, the contribution from a nucleophile should be minimal (see discussion below). Thus, it is unlikely that the observed inverse isotope effect on k_2 arises from the thiol group.

Interpretation of solvent isotope effects for enzymatic reactions can be complex, particularly in view of the multistep nature involving both binding and covalency changes. Caution should always be taken when analyzing and interpreting the data because of the possible general medium effects, viscosity, etc. in D_2O (Quinn & Sutton, 1991). In the case of the NAD-malic enzyme−catalyzed reaction, D_2O causes an inverse solvent isotope effect that is attributed to the difference in viscosity between H_2O and D_2O (Karsten et al., 1995). There is no commonly used microviscosogens that have no nucleophilic hydroxyl groups present. Compounds with nucleophilic hydroxyl groups have differential effects on the individual steps in reactions catalyzed by phosphatases. Further detailed and systematic investigation of the effect of viscosity on the PTPase-catalyzed reaction is needed. The results of solvent isotope effects will be discussed in the context of the nature of the transition states in noncatalyzed as well PTPase-catalyzed phosphate monoester hydrolysis.

Nature of the Transition State. Nonenzymatic hydrolysis of phosphate monoesters proceeds most easily at pH 4 where the predominate form corresponds to the monoanion. Hydrolysis of the phosphate monoester monoanions displays a small β_{lg} (−0.27 to −0.32), in accord with the departure of a neutral leaving group (Bunton et al., 1967; Kirby & Varvoglis, 1967). These data have been interpreted to imply a pre-equilibrium proton transfer to the bridge oxygen atom followed by phosphorus−oxygen (P−O) bond fission in the rate-limiting step. For leaving groups with pK_a <7, this proton transfer may become rate-limiting (Kirby & Varvoglis, 1967). More recent studies of model systems suggest that phosphoryl group trnasfer reactions involve an "exploded" metaphosphate-like transition state where bond formation to the incoming nucleophile is minimal and bond breaking between phosphorus and the leaving group is substantial (Bourne & Williams, 1984a; Skoog & Jencks, 1984; Herschlag & Jencks, 1989; and Cleland, 1990). As a result, there is a corresponding negative charge developing on the departing alcoholic or phenolic oxygen atom which can be stabilized by protonation, a positively charged group, or a metal ion. Stabilization of the buildup of negative charge on the leaving group is one of the potential mechanisms for stabilization of a dissociative transition state (Herschlag & Jencks, 1990).

The active form of the substrate for PTPases and the dual specificity phosphatases is phosphate monoester dianion (Zhang et al., 1994c; Denu et al., 1995b). The β_{lg} for the uncatalyzed hydrolysis of dianion is −1.27 (Kirby & Varvoglis, 1967), which is consistent with a highly dissociative transition state in which the P−O bond breaking is well

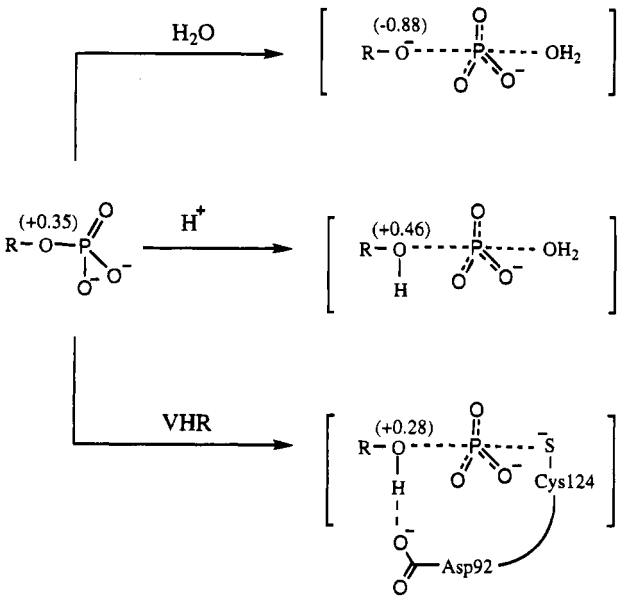

FIGURE 3: Transition-state structures of the spontaneous hydrolysis, the specific acid-catalyzed hydrolysis, and the VHR-catalyzed hydrolysis of the dianion. The effective charges on the leaving oxygen atom for each of the reactions represented in the figure were calculated according to Hall and Williams (1986). All effective charges are referred to the defined charge change of −1 in the standard phenol ionization equilibrium. The effective charge on the oxygen of the ionized and unionized phenol are defined to −1 and 0, respectively.

advanced. Recently, we have shown by measuring the heavy-atom kinetic isotope effects associated with the PTPase-catalyzed hydrolysis of *p*NPP, that the chemistry is rate-limiting and that the transition-state is also dissociative for the PTPase-catalyzed reaction (Hengge et al., 1995). Thus the small β_{lg} value observed for k_{cat}/K_m in the VHR-catalyzed phosphate monoester hydrolysis can be accounted for by the protonation of the leaving group, similar to the specific acid-catalyzed monoester hydrolysis in solution. Figure 3 compares the transition-state structures of the spontaneous, the specific acid-catalyzed, and the VHR-catalyzed hydrolysis of the dianion. It is apparent that the effective charge on oxygen for the VHR-catalyzed phosphoenzyme formation reaction is substantially more positive (+0.28) than the value that would be expected for a spontaneous hydrolysis reaction (−0.88). In fact, it is closer to the value observed for the acid-catalyzed hydrolysis reaction (+0.46). Thus the electronic requirements of the enzymatic phosphorylation are closer to those of the phosphate monoester hydrolysis catalyzed by the proton. Based on the structural and biochemical evidence discussed above, we propose that the considerable electrophilic catalysis in the VHR reaction is in fact due to the proton trnasfer from the putative general acid Asp92 to the leaving group. The principal question now that needs to be addressed is: where is the proton in the transition state?

Figure 3 is depicted with the proton almost completely transferred to the leaving oxygen and weakly hydrogen bonded to the general acid Asp92 in the transition state. The proton in the transition state cannot be shared equally between the general acid Asp92 and the phenolate oxygen. The reason is that the pK_a of the proton donor (7.2 for Asp92 in the enzyme−*p*NPP complex, Denu et al., 1995b) matches that of the acceptor (7.14 for *p*-nitrophenolate) in the transition state and such a hydrogen bond would produce a large normal solvent isotope effect due to the considerably less than unity fractionation factor (Quinn & Sutton, 1991). Specifically, we propose that the formation of the phosphoenzyme intermediate occurs with either rapid pre-equilibrium proton transfer to the bridging oxygen followed by P−O bond fission in the rate-limiting step, or that the proton trnasfer step is ahead of the P−O bond breaking thus resulting in an asymmetric transition state. Such a proposal is consistent with the near zero β_{lg} value observed for k_{cat}/K_m. It is also consistent with the inverse kinetic solvent isotope effect observed for the phosphorylation step (k_2). The inverse solvent isotope effect could simply be due to the fact that the acidity of acids is decreased two to three times in D_2O, and that the equilibrium concentration of the conjugate acid of the substrate is some 2 to 3 times higher in D_2O (Jencks, 1987). A chemical precedent for the pre-equilibrium proton transfer is the specific acid-catalyzed hydrolysis of phosphate monoesters (Kirby & Varvoglis, 1967). A solvent isotope effect of $k^{H_2O}/k^{D_2O} = 0.87$ was observed for the hydrolysis of methyl phosphate monoanion (Bunton et al., 1958), whereas a $k^{H_2O}/k^{D_2O} = 1.45$ was observed for the hydrolysis of 2,4-dinitrophenyl phosphate monoanion (Kirby & Varvoglis, 1967). These values are consistent with the proposal that the hydrolysis of monoanions involves a pre-equilibrium proton trnasfer to the bridge oxygen followed by P−O bond cleavage, whereas for good leaving groups such as 2,4-dinitrophenol, rate-limiting proton transfer is concurrent with P−O bond cleavage, resulting in a normal solvent isotope effect. The inverse solvent isotope effect could also be accounted for by the fractionation factor of the protonated phenol ester which should be similar to that of the hydronium ion (0.69, Quinn & Sutton, 1991). Finally, secondary ^{15}N isotope effects in the nitrogen atom of the leaving group, *p*-nitrophenol, which measure the extent of delocalization into the aromatic ring of the partial negative charge resulting from partial cleavage of the P−O bond in the transition state, indicate little charge delocalization into the aromatic ring for both the uncatalyzed monoanion hydrolysis and the PTPase-catalyzed hydrolysis of *p*NPP (Hengge & Cleland, 1990; Hengge et al., 1994, 1995). These results are consistent with either a pre-equilibrium or a concerted proton trnasfer to the bridging oxygen in the transition state of the P−O bond cleavage. A concerted proton trnasfer in the transition state would have produced a normal solvent isotope effect. An inverse solvent isotope effect observed for the phosphorylation step would be consistent with the pre-equilibrium mechanism.

Linear free-energy relationships for equilibrium constants of model phosphate monoesters indicate that the bridging phosphoryl oxygen behaves as if it has a positive charge of +0.35 relative to a protonated oxygen in a phenol (Figure 3 and Bourne & Williams, 1984b). Therefore, feeding a proton to an ester oxygen is not a favorable process in solution. Theoretical calculations suggest that a monoester protonated at the bridge position has no stability (Hengge & Cleland, 1990). However, it may be possible for such an "enforced" hydrogen bond to form in an enzyme system, since on an enzyme entities are held together, and the resulting entropic fixation and substrate destabilization contribute to enzyme catalysis. Once such a protonated species is formed, catalysis proceeds most efficiently. Indeed, the structure of PTP1B complexed with a peptide substrate (Jia et al., 1995) reveals that the phenolic oxygen of phosphotyrosine forms a

hydrogen bond with the corresponding general acid Asp181 even at pH 7.5 which is some distance from the pH optimum for catalysis (Zhang, 1995a). In addition to transition-state stabilization, an added advantage for the pre-equilibrium or the enforced hydrogen-bonding mechanism is that catalysis can also be realized through this destabilizing ground-state interaction between the bridging oxygen and the active-site general acid. Analogous destabilizations resulting from interactions between a metal ion or a hydrogen bond donor and the bridge oxygen are believed to operate in other protein enzymes as well as ribozymes (Narlikar et al., 1995). Furthermore, the hydrogen bond between the bridging oxygen and the general acid in the pre-catalytic complex also ensures the partitioning of the intermediate to favor the forward reaction. The pK_a values for the PTPases active-site thiol groups are low [4.7 for the *Yersinia* PTPase (Zhang & Dixon, 1993) and 5.6 for VHR (Denu et al., 1995b)]. In the metaphosphate-like transition-state (Figure 3), which is highly unstable, a strong electrophilic "pull" on the leaving group would be required for the productive forward reaction, since the conjugate acids of phenoxide and alkoxide generally have pK_a values much higher than 4.7−5.6.

After the formation of the phosphoenzyme intermediate, the hydrolysis of the intermediate would require water to attack the phosphorus atom, thus regenerating the active-site nucleophile and yielding the other product of the reaction, inorganic phosphate. Presumably, Asp92, which acts as a proton donor in the phosphorylation step (k_2), would play the role of a general base abstracting a proton from the attacking water nucleophile in the transition state of the dephosphorylation step (k_3). The solvent isotope effect for this step is low (1.15). This would not be surprising if one recalls that very small dependencies ($\beta_{nuc} = 0$ to 0.2) of the rate of phosphoryl transfer on the nucleophilicity (pK_a) of the attacking nucleophiles are observed (Kirby & Varvoglis, 1968; Bourne & Williams, 1984a; Skoog & Jencks, 1984). This implies that there is only a small amount of bond formation to the incoming nucleophile and is consistent with a highly dissociative transition state. If we assume that the transition state for the hydrolysis of the thiophosphate intermediate is similar to that of the phosphorylation step, the small solvent isotope effect is understandable because bond formation between the phosphorus atom and the nucleophilic water is minimal in the transition state. In other words, minimal water activation is needed for the hydrolysis step.

Conclusions. In this paper, we have probed the active-site substrate specificity of the human dual-specificity phosphatase, VHR. Unlike PTPases which exhibit intrinsically different activities toward aryl and alkyl phosphates, we show that VHR hydrolyzes small aryl phosphates and alkyl phosphates with similar turnover numbers. From the results of both leaving-group dependencies of steady-state kinetic parameters and pre−steady-state burst kinetics, we conclude that the rate-limiting step for the VHR-catalyzed hydrolysis is the breakdown of the phosphoenzyme intermediate. The reason for VHR's "promiscuity" toward small phosphate monoesters may be its unusual active-site property for effective electrophilic catalysis of the phosphorylation step. We propose that this effective electrophilic catalysis is achieved by an unsynchronized, early proton transfer to the bridge oxygen in the transition state of the P−O bond-breaking process. Such a proton trnasfer provides the driving force for the enzyme to go through a dissociative pathway.

ACKNOWLEDGMENT

We thank Dr. Robert Van Etten for an initial sample of 5-phenylpentyl phosphate and Dr. John Blanchard for the use of the stopped-flow instrument. We also thank Drs. W. W. Cleland, V. Schramm, A. Hengge, and D. Herschlag for helpful discussions.

REFERENCES

Aroca, P., Bottaro, D. P., Ishibashi, T., Aaronson, S. A., & Santos, E. (1995) *J. Biol. Chem. 270*, 14229−14234.
Ballinger, P., & Long, F. A. (1960) *J. Am. Chem. Soc. 82*, 795−798.
Black, M. J., & Jones, M. E. (1983) *Anal. Biochem. 135*, 233−238.
Bourne, N., & Williams, A. (1984a) *J. Am. Chem. Soc. 106*, 7591−7596.
Bourne, N., & Williams, A. (1984b) *J. Org. Chem. 49*, 1200−1204.
Bunton, C. A., Llewellyn, O. R., Oldham, K. G., & Vernon, C. A. (1958) *J. Chem. Soc.* 3574−3587.
Bunton, C. A., Fendler, E. J., Humeres, E., & Yang, K.-U. (1967) *J. Org. Chem. 32*, 2806−2811.
Charbonneau, H., & Tonks, N. K. (1992) *Annu. Rev. Cell Biol. 8*, 463−493.
Cho, H., Krishnaraj, R., Kitas, E., Bannwarth, W., Walsh, C. T., & Anderson, K. S. (1992) *J. Am. Chem. Soc. 114*, 7296−7298.
Cleland, W. W. (1990) *FASEB J. 4*, 2899−2905.
Denu, J. M., Zhou, G., Wu, L., Zhao, R., Yuvaniyama, J., Saper, M. A., & Dixon, J. E. (1995a) *J. Biol. Chem. 270*, 3796−3803.
Denu, J. M., Zhou, G., Guo, Y., & Dixon, J. E. (1995b) *Biochemistry 34*, 3396−3403.
Fischer, E. H., Charbonneau, H., & Tonks, N. K. (1991) *Science 253*, 401−406.
Gautier, J., Solomon, M. J., Booher, R. N., Bazan, J. F., & Kirschner, M. W. (1991) *Cell 67*, 197−211.
Guan, K. L., & Dixon, J. E. (1990) *Science 249*, 553−556.
Guan, K. L., & Dixon, J. E. (1991) *J. Biol. Chem. 266*, 17026−17030.
Guan, K. L., Broyles, S. S., & Dixon, J. E. (1991) *Nature 350*, 359−362.
Hall, A. D., & Williams, A. (1986) *Biochemistry 25*, 4784−4790.
Hammes, G. G., & Schimmel, P. R. (1970) in *The Enzymes* (Boyer, P. D., Ed.) Vol. II, p 67, Academic Press, New York.
Hengge, A. C., & Cleland, W. W. (1990) *J. Am. Chem. Soc. 112*, 7421−7422.
Hengge, A. C., Edens, W. A., & Elsing, H. (1994) *J. Am. Chem. Soc. 116*, 5045−5049.
Hengge, A. C., Sowa, G., Wu, L., & Zhang, Z.-Y. (1995) *Biochemistry* (in press).
Herschlag, D., & Jencks, W. P. (1989) *J. Am. Chem. Soc. 111*, 7579−7586.
Herschlag, D., & Jencks, W. P. (1990) *Biochemistry 29*, 5172−5179.
Ishibashi, T., Bottara, D. P., Chan, A., Miki, T., & Aaronson, S. A. (1992) *Proc. Natl. Acad. Sci. U.S.A. 89*, 12170−12174.
Jencks, W. P. (1987) *Catalysis in Chemistry and Enzymology*, p 250, Dover, New York.
Jia, Z., Barford, D., Flint, A. J., & Tonks, N. K. (1995) *Science 268*, 1754−1758.
Karsten, W. E., Lai, C.-J., & Cook, P. F. (1995) *J. Am. Chem. Soc. 117*, 5914−5918.
Kirby, A. J., & Varvoglis, A. G. (1967) *J. Am. Chem. Soc. 89*, 415−423.
Kirby, A. J., & Varvoglis, A. G. (1968) *J. Chem. Soc. B*, 135−141.
Klinman, J. P. (1977) *Adv. Enzymol. 46*, 415−494.
Narlikar, G. J., Gopalakrishnan, V., McConnell, T. S., Usman, N., & Herschlag, D. (1995) *Proc. Natl. Acad. Sci. U.S.A. 92*, 3668−3672.
Perrin, D. D. (1965) *Dissociation Constants of Organic Bases in Aqueous Solution*, p 406, Butterworths, London.

Quinn, D. M., & Sutton, L. D. (1991) in *Enzyme Mechanism from Isotope Effects* (Cook, P. F., Ed.) pp 73−126, CRC Press, Boca Raton, FL.
Schowen, K. B., & Schowen, R. L. (1982) *Methods Enzymol. 87*, 551−606.
Skoog, M. T., & Jencks, W. P. (1984) *J. Am. Chem. Soc. 106*, 7597−7606.
Sparks, J. W., & Brautigan, D. L. (1985) *J. Biol. Chem. 260*, 2042−2045.
Stuckey, J. A., Fauman, E. B., Schubert, H. L., Zhang, Z.-Y., Dixon, J. E., & Saper, M. A. (1994) *Nature 370*, 571−575.
Sun, H., Charles, C. H., Lau, L. F., & Tonks, N. K. (1993) *Cell 75*, 487−493.
Tonks, N. K., Diltz, C. D., & Fischer, E. H. (1988) *J. Biol. Chem. 263*, 6731−6737.
Walton, K., & Dixon, J. E. (1993) *Annu. Rev. Biochem. 62*, 101−120.
Ward, Y., Gupta, S., Jensen, P., Wartmann, M., Davis, R. J., & Kelly, K. (1994) *Nature 367*, 651−654.
Wo, Y.-Y. P., Zhou, M.-M., Stevis, P., Davis, J. P., Zhang, Z.-Y., & Van Etten, R. L. (1992) *Biochemistry 31*, 1712−1721.
Zhang, Z.-Y. (1995a) *J. Biol. Chem. 270*, 11199−11204.
Zhang, Z.-Y. (1995b) *J. Biol. Chem. 270*, 16052−16055.
Zhang, Z.-Y., & Van Etten, R. L. (1990) *Arch. Biochem. Biophys. 282*, 39−49.
Zhang, Z.-Y., & Van Etten, R. L. (1991a) *J. Biol. Chem. 266*, 1516−1525.
Zhang, Z.-Y., & Van Etten, R. L. (1991b) *Biochemistry 30*, 8954−8959.
Zhang, Z.-Y., & Dixon, J. E. (1993) *Biochemistry 32*, 9340−9345.
Zhang, Z.-Y., Wang, Y., & Dixon, J. E. (1994a) *Proc. Natl. Acad. Sci. U.S.A. 91*, 1624−1627.
Zhang, Z.-Y., Wang, Y., Wu, L., Fauman, E., Stuckey, J. A., Schubert, H. L., Saper, M. A., & Dixon, J. E. (1994b) *Biochemistry 33*, 15266−15270.
Zhang, Z.-Y., Malachowski, W. P., Van Etten, R. L., & Dixon, J. E. (1994c) *J. Biol. Chem. 269*, 8140−8145.
Zhou, Z., Denu, J. M., Wu, L., & Dixon, J. E. (1994) *J. Biol. Chem. 269*, 28084−28090.

BI951727G